Productivity of mixed kelp communities in an Arctic fjord exhibit tolerance to a future climate

Cale A Miller, Frédéric Gazeau, Anaïs Lebrun, Jean-Pierre Gattuso, Samir Alliouane, Pierre Urrutti, Robert W Schlegel, Steeve Comeau

Science of the Total Environment 930 (2024) 172571

Contents lists available at ScienceDirect

Science of the Total Environment

journal homepage: www.elsevier.com/locate/scitotenv

Productivity of mixed kelp communities in an Arctic fjord exhibit tolerance to a future climate

Cale A. Miller [a,b,*], Frédéric Gazeau [a], Anaïs Lebrun [a], Jean-Pierre Gattuso [a,c], Samir Alliouane [a], Pierre Urrutti [a], Robert W. Schlegel [a], Steeve Comeau [a]

[a] Sorbonne Université, CNRS, Laboratoire d'Océanographie de Villefranche, 181 chemin du Lazaret, 06230 Villefranche-sur-Mer, France
[b] Department of Earth Sciences, Geosciences, Utrecht University, Utrecht, the Netherlands
[c] Institute for Sustainable Development and International Relations, Sciences Po, 27 rue Saint Guillaume, 75007 Paris, France

HIGHLIGHTS

- Future climate change in Arctic fjord systems manifests as multiple perturbations
- Arctic kelp communities were exposed to warming, freshening, and reduced light
- Net community production by mixed kelp communities was most affected by light
- Model predictions suggest mixed kelp communities are net autotrophic during summer
- Summer net productivity by Arctic kelp appears tolerant to future multi-stressors

GRAPHICAL ABSTRACT

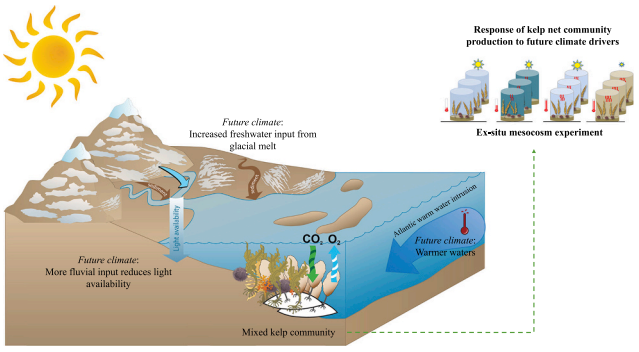

ARTICLE INFO

Editor: Olga Pantos

Keywords:
Kelp
Arctic
Multi-stressors
Climate change
Net community production
Compensation irradiance

ABSTRACT

Arctic fjords are considered to be one of the ecosystems changing most rapidly in response to climate change. In the Svalbard archipelago, fjords are experiencing a shift in environmental conditions due to the Atlantification of Arctic waters and the retreat of sea-terminating glaciers. These environmental changes are predicted to facilitate expansion of large, brown macroalgae, into new ice-free regions. The potential resilience of macroalgal benthic communities in these fjord systems will depend on their response to combined pressures from freshening due to glacial melt, exposure to warmer waters, and increased turbidity from meltwater runoff which reduces light penetration. Current predictions, however, have a limited ability to elucidate the future impacts of multiple-drivers on macroalgal communities with respect to ecosystem function and biogeochemical cycling in Arctic fjords. To assess the impact of these combined future environmental changes on benthic productivity and resilience, we conducted a two-month mesocosm experiment exposing mixed kelp communities to three future conditions comprising increased temperature (+ 3.3 and + 5.3°C), seawater freshening by ~ 3.0 and ~ 5.0 units (i.e., salinity of 30 and 28, respectively), and decreased photosynthetically active radiation (PAR, - 25 and - 40 %). Exposure to these combined treatments resulted in non-significant differences in short-term productivity, and a tolerance of the photosynthetic capacity across the treatment conditions. We present the first robust estimates of mixed kelp community production in Kongsfjorden and place a median compensation irradiance of ~12.5

* Corresponding author at: Vening Meinesz building A, Princetonlaan 8a, 3584 CB Utrecht, The Netherlands.
E-mail address: c.a.miller@uu.nl (C.A. Miller).

https://doi.org/10.1016/j.scitotenv.2024.172571
Received 1 September 2023; Received in revised form 22 March 2024; Accepted 16 April 2024
Available online 23 April 2024

mmol photons m^{-2} h^{-1} as the threshold for positive net community productivity. These results are discussed in the context of ecosystem productivity and biological tolerance of kelp communities in future Arctic fjord systems.

1. Introduction

The accelerated rate of Arctic warming is often expressed as a way to convey the urgency of a rapidly changing climate. While atmospheric warming of the Arctic is occurring at a rate 4× faster than the rest of the world, such proclamations overlook the intricacies and nuances of climate change drivers in disparate Arctic biomes, particularly in fjord systems (Carvalho and Wang, 2020; Rantanen et al., 2022; Schlegel et al., 2023). In the pan-Arctic, the mean sea surface temperature (SST) increase over the past two decades has been nearly identical to that of the rest of the globe (Chen et al., 2019; Fox-Kemper et al., 2021). This similarity, however, is due to the heterogeneity of the pan-Arctic, which encompasses large swaths of polar waters bordering Russia and Canada that display a meager decadal warming trend of <0.2 °C $decade^{-1}$ (Carvalho and Wang, 2020). This contrasts with warming trends in the European Arctic, as the complexity of Arctic hydrology is realized in the Norwegian and East Greenland Seas, which show a mean SST warming rate between 0.15 and 0.5 °C $decade^{-1}$ in late winter and summer, respectively (Meredith et al., 2019). Within this region lies the west coast of the Svalbard archipelago, which has experienced a steadily warming SST for the past two decades due to a more frequent influx of warm Atlantic water throughout the year (Tverberg et al., 2019; Skogseth et al., 2020). This "Atlantification" has led to rapid loss of glacial mass and the retreat of sea terminating glaciers in NW Svalbard (Asbjørnsen et al., 2020; Morris et al., 2020). The conglomeration of increasing SST and glacial retreat—along with associated freshwater influx—are expected to modify fjord hydrography potentially enhancing retention of freshwater and inducing an earlier phytoplankton bloom season (Husum et al., 2019; Torsvik et al., 2019). Although, the characteristics of these changes to stratification and primary production within the fjord will depend on the type of meltwater plume (land or sea derived) coming from glaciers (Meire et al., 2023). These modifications to the physicochemical environment have been described as a potential darkening of Svalbard fjords due to the increased heat retention, ice-loss, and runoff from proglacial streams that attenuate the penetration of photosynthetically active radiation (PAR) (Torsvik et al., 2019; Konik et al., 2021; van de Poll et al., 2021). The forthcoming interaction of these changes are difficult to quantify with respect to how these shifts may affect the function and resilience of biological communities—specifically benthic communities.

Large brown seaweeds, colloquially referred to as kelp, are a dominant group of macroalgae that exist on hard bottoms throughout the shallow depths of the nearshore Arctic (e.g., fjords). Kelp are dominated by the order Laminariales and are abundant throughout the Arctic region, including within fjord systems such as Kongsfjorden, Svalbard (Hop et al., 2012; Alongi, 2018; Wernberg et al., 2019; Goldsmit et al., 2021). They create biogenic habitats that provide a functional ecosystem role with respect to shelter, food source, and carbon cycling in the Arctic (Włodarska-Kowalczuk et al., 2009; Filbee-Dexter et al., 2019; Fredriksen et al., 2019). Many macroalgae in the Arctic are thought to have a boreal origin surviving in refugia zones during previous glacial periods resulting in a contemporary, diverse mixed community forest system (Bringloe et al., 2020). Thus, the species of kelp within the Arctic region are also abundant in sub-Arctic regions, and display varying degrees of inter-species tolerance to warming, decreased irradiance, and freshening (Filbee-Dexter et al., 2019; Lebrun et al., 2022 and references therein). Recent modeling studies even suggest an overall net gain of macroalgae biomass throughout the Arctic due to warmer temperatures (especially in winter) and reduced sea ice cover and scouring from glacial calving (Krause-Jensen et al., 2020; Assis et al., 2022).

Many of the ecological functions provided by Arctic kelp communities can be understood through the lens of biogeochemical cycling, which involves the metabolic processes of the system related to nutrient uptake and retention within the habitat, as well as carbon cycling (Abdullah et al., 2017; Filbee-Dexter et al., 2018). With the projected future increase in kelp biomass and coverage, it is important to consider the role kelp communities may have in biogeochemical cycling in the Arctic, particularly regarding benthic primary production. Recent estimates suggest benthic primary production currently accounts for ~25 % of ecosystem production for outer fjord regions (Attard et al., 2016). This estimate may increase with the predicted expansion of kelp, shifting the balance of benthic-pelagic coupling and benthic primary production to changes in ecosystem function. From a future pan-Arctic perspective, the environmental drivers that will modify the physicochemical environment portray a positive prospect for Arctic kelp, but this potentially overlooks smaller scale changes at the community level.

One of the most impactful drivers of climate change in the Arctic fjord of Kongsfjorden relates to changes in the underwater light climate, which is hypothesized as the cause for the observed shoaling of kelp depth distribution in the region (Bartsch et al., 2016). Changes in the underwater light climate due to the spatial extent and turbidity of sediment plumes at different stages of glacial retreat and water mass mixing show that land terminating glaciers in Kongsfjorden are responsible for the most deteriorated underwater light conditions compared to coast water and sea-terminating glaciers, which correlates to a vertical depth limit for kelp (Niedzwiedz and Bischof, 2023). Given that the underwater light climate is one of the main drivers for kelp depth distribution and production (Fragkopoulou et al., 2022; Niedzwiedz and Bischof, 2023), quantifying the consortium of climatic drivers including light climate becomes essential for understanding the role of benthic primary production in fjord systems now and in the future. While many studies have observed an independent response of individual kelp physiological function to warming, freshening, and irradiance in the Arctic (Filbee-Dexter et al., 2019; Lebrun et al., 2022; Niedzwiedz and Bischof, 2023), a mixed kelp community response remains equivocal.

To assess the metabolic response and production of mixed kelp communities inhabiting an Arctic fjord to future climate drivers, we employed a novel multi-stressor experimental system manipulating temperature and salinity in real-time combined with modifications to incoming irradiance over a two-month manipulative experiment in Kongsfjorden, Svalbard. Weekly ex-situ community level incubations were performed to test (1) how combinations of warming, freshening, and decreased irradiance (mimicking increased turbidity) may affect kelp community productivity, and (2) how the independent effects of warming impact community metabolism. The aim of the presented study depicts the tolerance of Arctic kelp communities to future climate drivers and estimates their current metabolic capacity as it relates to net community productivity (NCP).

2. Materials and methods

2.1. Kongsfjorden system

Kongsfjorden is a glacial fjord situated on the west coast of Svalbard (78°59′ N, 11–12° E) which is subject to warm and salty, North Atlantic water intrusion to the West Spitsbergen Current. Temperatures in the fjord have been warming at rate of 0.11 °C y^{-1} during the warm months (Sept. – Nov.) over the past 2 decades (Hop et al., 2019). During the summer melt season, brown water plumes form at the surface, which are generated by sub-glacial discharge at the terminus of several tidewater

glaciers causing buoyant plumes to rise to the surface (Hegseth et al., 2019).

The temperature and salinity conditions in Kongsfjorden measured at the COSYNA Underwater Observatory (depth of 10 m) recorded monthly median values from 2015 to 2021 in winter and summer of - 0.1 °C and 6.1 °C, with salinity from 35 to 33.3 in spring and autumn, respectively (Gattuso et al., 2023). Further measurements of temperature, salinity, and PAR can be found on the COSYNA data portal site (https://dashboard.awi.de/?dashboard=3865) hosted by AWIPEV (Alfred Wegener Institute and Institute Paul Émile Victor). The nearshore shallow waters (< 12 m) of Kongsfjorden are oversaturated seasonally with respect to aragonite, where pH ranges between 8.0 and 8.2; however, acidification is expected to increase as a result of progressive glacial melt and a decrease in biological carbon uptake resulting from diminished nutrient input due to intruding warmer water masses (Fransson et al., 2016; Gattuso et al., 2023). These fjord conditions have been robustly represented in the experimental design described below.

2.2. Experimental logistics and design

The ex-situ perturbation experiment on mixed kelp communities was conducted on an outside platform in Ny-Ålesund, Svalbard, ~ 12 m from the shoreline. Kelps and associated fauna were collected in Kongsfjorden, Svalbard, at either Hansneset (78°59.101′ N, 11°57.793′ E), or the Old Pier (78°55′49.20′N, 11°55′10.59′E) at an average depth of 4.5 m by the AWI (Alfred Wegener Institute, Germany) dive team in late June 2021. Organisms were placed in holding tanks with ambient flow-through seawater for no >12 d prior to the start of the experiment. The three most abundant kelp species in Kongsfjorden were targeted for collection: *Alaria esculenta*, *Saccharina latissima*, and *Laminaria digitata*, along with an assortment of benthic fauna comprising sea urchins (*Strongylocentrotus pallidus*, *Strongylocentrotus droebachiensis*), snails (*Margarites* spp.), and brittle stars (*Ophiopholis aculeata*). A total of 142 kelp sporophytes ranging in size from 50 to 250 cm were collected in order to replicate the densities and diversity found at 7–10 m depth in a 1 m^2 plot equating to a total fresh weight (fw) of ~4 kg of kelp (Table 1; Hop et al., 2012). Targeted fauna biomass for a 1 m^2 plot were aligned to estimates from Paar et al. (2019), but only comprised the species listed above at a fw of ~400 g for sea urchins and < 150 g for snails and brittle stars at the start of the experiment.

A fractional factorial design was employed to expose benthic kelp communities in triplicate to three different treatment conditions within 12 opaque fiberglass mesocosms, each with a volume of 1 m^3 (~ 1.2 m in height and a mean diameter of 1.1 m). The treatments were designed to represent expected future conditions in the fjord under the projected climate change scenarios SSP2–4.5 and SSP5–8.5. These were discernible as three driving factors (1) increased temperature, (2) increased freshening from glacial retreat, and (3) attenuated light from increased fluvial material deposited by sub- and proglacial streams (Fig. 1). The first treatment (MSM) recognized moderate future change (SSP2–4.5) as an offset from ambient conditions at a 10 m depth, where temperature was warmed to +3.3 °C, salinity decreased between 2.5 and 3.0 units, and irradiance was attenuated by a 25 % mean value. The second treatment (MSH) manipulated the same factors to a higher degree offset (SSP5–8.5) from ambient conditions where temperature was warmed to +5.3 °C, salinity decreased between 5.0 and 5.5. units, and irradiance was attenuated by a 40 % mean value. The third treatment scenario (HT) was a warming only condition of +5.3 °C above ambient (SSP5–8.5).

Table 1
Sporophyte distribution per mesocosm with total fresh weight per species at T_0 and T_F. Numbers 1–3 refer to each replicate.

	Saccarina Latissima	*Alaria esculenta*	*Laminaria digitata*		
Mesocosm	Sum fresh weight (g)	Sum fresh weight (g)	Sum fresh weight (g)	T_0 Sum total (g)	T_f Sum total (g)
Cntrl. 1	1518	980	1536	4034	4046
Cntrl. 2	1442	994	1664	4100	4088
Cntrl. 3	1488	954	1656	4098	4022
MSM 1	1628	1150	1564	4342	4006
MSM 2	1516	964	1458	3938	3624
MSM 3	1520	1110	1522	4152	3768
MSH 1	1530	1014	1588	4132	3976
MSH 2	1514	972	1516	4002	3424
MSH 3	1528	1090	1580	4198	3662
HT 1	1602	1058	1484	4144	4136
HT 2	1486	1166	1526	4178	3678
HT 3	1442	996	1552	3990	3710

The experimental system was regulated by a novel temperature and salinity perturbation system which has been thoroughly described in Miller et al. (2024). Briefly though, the applied temperature anomalies of +3.3 and 5.3 °C were programmed as offset values from a dynamic control that followed measured in-situ fjord conditions (salinity, temperature, and PAR) at a 10 m depth recorded by the AWIPEV FerryBox part of the COSYNA underwater observatory. Water was pumped from a 10 m depth offshore to the Kings Bay marine laboratory where it was split into 3 sub-header tanks which either, warmed, chilled or left seawater unmodified before exiting a pipping manifold which autonomously regulated the mixing of warmed, chilled, or ambient seawater. Each treatment condition, including the control, was regulated using a series of automated regulator valves that mixed incoming flows of ambient, warmed ambient, and chilled ambient seawater with freshwater—when applicable—in specific volumetric proportions to achieve setpoint conditions. This was done by continuously (several measurements per minute) measuring the temperature and salinity in each mesocosm and transmitting the recorded data to a local network and custom designed computer application that monitored and controlled the flow and mixing of each source water inlet. Incoming irradiance was measured in each mesocosm by a PAR logger (Odyssey©) fixed to a centered PVC stand raising the logger to the top of the mesocosm at a vertical orientation. The control condition simulated a depth of 10 m using light and spectrum filters (Lee© Filters) adhered to acrylic covers fixed to a fiber glass ring that was set on top of each mesocosm. For the MSM and MSH treatments, additional light filters were placed on top of the spectral filters to achieve the mean 25 and 40 % attenuation targets.

2.3. Sampling and procedure

Each mesocosm was equipped with an in-situ optical oxygen (O_2) sensor (Aqualabo, PODOC), temperature-conductivity probe (Aqualabo, PC4E), PAR logger, and a 12 W wave pump (Sunsun© JVP-132). A total of 12–14 kelp sporophytes were evenly distributed according to weight and length differences across each mesocosm and attached by an intact holdfast to small stones using weaved twine to simulate natural substrate attachment. Before distributing individual kelp into each mesocosm, initial length, fresh weight (fw), and a hole punch 2 cm above the base of the meristem juncture with the stipe was made in order to monitor growth during the experiment. The results of this growth data can be found in Lebrun et al. (2023). Upon cataloging each metric and hole punch, the kelps were randomly distributed (considering collection site) into each mesocosm. This marked the start of the experiment on 2021-07-03 which began with a 7 d 'acclimation' period where all mesocosms received a continuous flow of ambient seawater.

Kelp community metabolism and productivity were determined by measuring oxygen evolution in each mesocosm after filling them to the rim, causing seawater to spill out the sides of the top cover. This left no headspace in the mesocosms, thus avoiding any potential air-water gas exchange. Once completely filled, 3 h incubations were performed by cutting the inflow and stopping the outflow. The internal wave pump ensured homogeneity and mixing of the water inside each mesocosm. A total of 12 closed incubations were performed over the 54 d experiment. The first five incubations were conducted during the ambient 'acclimation' period (every 1–2 d) while the following seven incubations

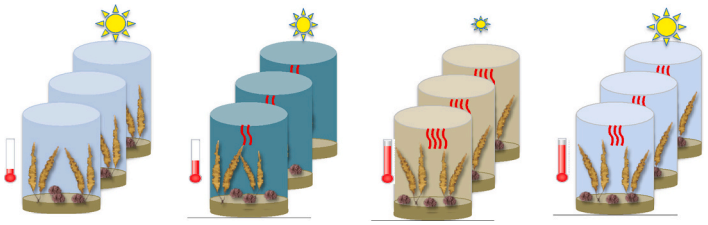

	CNTRL. 1 – 3	MSM 1 – 3	MSH 1 – 3	HT 1 – 3
Temperature	Ambient	+ 3.3 °C	+ 5.3 °C	+ 5.3 °C
Salinity	Ambient	Δ 2.5 – 3.0 y = 0.546*T + 0.490	Δ 5.0 – 5.5 y = 0.877*T + 0.089	Ambient
PAR	Ambient	~ 25% < ambient	~ 40% < ambient	Ambient

Fig. 1. Diagram of experimental design with treatment descriptions as multi-stressor medium (MSM), multi-stressor high (MSH), high temperature (HT), and a control (CNTRL.). All manipulated conditions followed the real-time measured ambient conditions in the fjord and nature light cycle.

(6–12) occurred weekly, while at target conditions. On the final day of the 'acclimation' period, one 4 h dark incubation was performed by placing three layers of black plastic sheets over the top of each mesocosm. On 2021-07-10, temperature was adjusted daily by programming a new setpoint in the software interface of the perturbation system to create a linear increase to the final target conditions achieved on 2021-07-16. This was an increase of 0.55 °C d^{-1} for the MSM treatment and 0.88 °C d^{-1} for MSH and HT treatments. Incubations occurred at different 3 h periods during the entire experimental period to compensate for uneven cloud cover over the experimental platform. The oxygen sensor in each mesocosm recorded minutely changes in O_2 concentration that were used to estimate net production of the simulated community. Incubations were terminated by restoring open-flow and turning the automated perturbation system back on to continue the regulation of each experimental condition in the mesocosms. Regular maintenance was performed by cleaning the walls of each mesocosm and its sensors (i.e., oxygen sensor, PAR logger, and temperature-conductivity probe) of epiphytes. Sensors were cleaned every 2 to 3 d, and again directly before performing an incubation.

Tissue sampling and dry weight (dw) determination for all 142 sporophytes was conducted the day after the final incubation (2021-08-26) and was completed on 2021-08-29. The breakdown of the experiment occurred over 3 d due to the number of sporophytes that needed to be processed. Each day during breakdown, 1 replicate for each treatment was terminated ensuring any added variance introduced over the 3 days needed to process all kelp samples was captured within a treatment. Measurements were made for total length (Lebrun et al., 2023) and fw, with and without the stipe. Each kelp was then dried for at least 72 h at 60 °C. A fw to dw conversation factor was calculated for each species by pooling all sporophytes of a single species to construct the correlation (Table S1). The total biomass of each mesocosm was calculated at the end of the experiment in order to quantify potential gain or loss, and a linear interpolation was applied between the T_0 and T_F biomass measurements. The interpolated values were used to estimate biomass at any given time point in each mesocosm as real measurements were not available.

Metabolic carbon cycling by kelp communities was assessed by collecting discrete bottle samples of pH_T (total scale) and total alkalinity (A_T) before and after an incubation in order to constrain the carbonate system and calculate changes in total inorganic carbon (C_T). The samples were stored in 300 ml BOD (biological oxygen demand) and 250 ml HDPE (high-density polyethylene) bottles for pH_T and A_T, respectively. pH_T was measured in a 30 ml cylindrical cell using a Cary 60 (Agilent Technologies) spectrophotometer and purified *m*-cresol purple as an indicator dye (Dickson et al., 2007). Triplicate or duplicate analytical replicates were measured for each collected sample within 3 h of bottling. A_T was measured using an open-cell titration method (Dickson et al., 2007) on a Metrohm888 Titrando with triplicate or duplicate runs (50 ml) performed on the same sample bottle as analytical replication. Several samples of certified reference material (purchased from Andrew Dickson, Scripps Institute of Oceanography, USA) were processed haphazardly throughout the experimental period to ensure proper accuracy by the titrator (within ±4 μmol kg^{-1}). The carbonate system parameters were derived using CO2SYS (Matlab v3.1.1; Sharp et al., 2021) with the carbonic acid dissociation constants of Sulpis et al. (2020), bisulfate constant from Dickson (1990), fluoride from Perez and Fraga (1987), and the boron/chlorinity ratio of Uppström (1974).

2.4. Statistical approach and modeling

Erroneous values of PAR were filtered by percentile (< 0.01 % at either end). The measured outliers occurred due to the removal of the mesocosm covers during cleaning, or from fronds passing over the PAR logger. Short instances of erroneous values were removed as described above and linearly interpolated. Longer periods of erroneous values were either removed completely or estimated by taking the mean value of the other two replicate mesocosms when appropriate (e.g., an observed minimal difference that ranged from 0.07 to 15.3 μmol photons m^{-2} s^{-1} across replicates during a 24 h period prior to when the estimated value was used).

Determination of NCP was quantified by calculating P—I (photosynthesis-irradiance) curves or slopes from O_2 evolution in each mesocosm. Three, hourly, NCP rates were derived for each mesocosm per incubation in order to account for any changes in PAR over the 3 h duration. A hyperbolic tangent function was used to describe the P—I curves. A linear function was used when PAR levels were below saturating irradiance, and when rates fell along the tangent line of the curve. The compensation irradiance point (I_c) and initial slope (α) were determined from either the hyperbolic tangent or linear model. Random factors such as 'Time of Day' and 'Day of Year' were considered as confounding variables that could affect NCP and, thus, integrated into the analysis.

Rates of NCP were compared for every treatment condition using a stepwise linear model with covariates, PAR, 'Time of day', and 'Day of the year' to determine the response of mixed kelp net community productivity. The integrated sum of all calculated rates (i.e., sum of all hourly rates for each treatment) was determined across treatments using a Wilcoxon rank sum with an applied Bonferroni-Holm multiple comparisons correction. This analysis was repeated using the projected linear model estimates of hourly NCP with select PAR values identified

as a 'typical light day'. The 'typical light day' PAR values were selected haphazardly from the measured PAR in the control treatment for an entire day when hourly PAR < 45 mmol photons m^{-2} h^{-1}. One day was selected for each week from 18 July to 19 August. The 'typical light day' (5 days in total) represented the majority of observed hourly PAR measurements recorded during this time period of the experiment.

The estimated NCP was derived from a single rate model determined by pooling the measured rates of hourly NCP across all treatments. This was done using a modified hyperbolic tangent model that incorporated 'Time of day' as an additional variable. 'Time of day' was applied as a linear negative correlation scaler as:

$$NCP = P_{max} tanh\left(\frac{\alpha I}{P_{max}}\right) + R_d \times ToD, \quad (1)$$

where P_{max} is the maximum NCP (μmol O_2 g dw^{-1} h^{-1}), I is the PAR (mmol photons m^{-2} h^{-1}), α is the initial slope of the curve (μmol O_2 g dw^{-1} h^{-1}(mmol photons m^{-2} h^{-1})$^{-1}$), R_d is the dark respiration rate (μmol O_2 g dw^{-1} h^{-1}), and *ToD* is the 'Time of day' (decimal hour in a day). The pooling of all measured rates of hourly NCP was justified due to the lack of significant differences observed across treatments compared to the control.

The NCP estimate is representative of kelp community productivity in Kongsfjorden at the simulated 10 m depth and was used to predict daily net community production. Calculating the daily net community production was realized by using the unmanipulated PAR values from one of the control mesocosms (the 3rd control replicate) and applying these values to the model function as the representative in-situ PAR at a 10 m depth. Given that each mesocosm represented the biomass in a m^{-2} plot, the mean biomass per day across all mesocosms was applied to convert biomass to a m^{-2} area of production (mmol O_2 m^{-2} d^{-1}).

The derived carbonate chemistry parameters were considered valid only when discrete pH_T and A_T bottle samples were filtered to remove outliers within analytical replicates. A routine outlier removal process was applied using the 'isoutlier' function in Matlab (V. 2022a) with a selected 'median' method and threshold factor of 2. For instances when there was lack of agreement (i.e., each measured A_T value had differences >10 μmol kg^{-1} from one another) amongst analytic replicates, the entire sample was removed. This was not needed for the measured pH_T samples. When applicable, C_T was calculated from the average A_T and pH_T values by treatment for incubations 6–12.

3. Results

3.1. Experimental system function

Over the 54 d experiment, the regulation of temperature and salinity in each mesocosm was well maintained (Figs. S1, S2). Deviations >0.5 salinity or 0.5 °C between the measured values in each mesocosm and the setpoint value during incubations were absent except for salinity, which deviated ~1.2 from the setpoint on 26-08-2021 for replicates 2 and 3 of the MSM treatment (Fig. S2). Overall, the variability in the experimental conditions was minimal or negligible during incubation periods.

Measurements of the daily integrated PAR displayed robust separation of the manipulated irradiance throughout the experimental period (Fig. S3). The mean proportional decrease between the daily integrated PAR for the MSM treatment and control condition was 0.289, 0.217, and 0.204 across replicates. For the MSH treatment, the daily integrated PAR displayed a mean proportional decrease from the control of 0.364, 0.365, and 0.349 for each replicate.

The T_f values of kelp biomass (fw) decreased in all mesocosms with the exception of 1 replicate in the control condition (Table 1). In total, 7 kelp where found completely senesced (frond gone, with only mid-rib remaining) or dead. This was a total of 4 kelps across the MSM replicates, 2 kelps across the MSH treatments, and 1 kelp in the HT treatment. Across the control replicates, 2 kelp fronds where found detached from the stipe. Dead urchins, brittle stars, and snails were found in all mesocosms, reducing the total biomass of fauna in each tank from ~10 % fw at the start of the experiment to an estimated 5–7 % based on empty urchin tests, which was quantifiable to a loss of 35–40 % total biomass from T_0 urchin biomass.

3.2. Response of NCP to treatment conditions

Hourly rates of NCP across all treatments and incubations displayed non-significant differences from the control as a function of irradiance (Fig. 2). Incoming PAR was greatest at the beginning of the experiment in early July when all mesocosms were supplied with the same, unmanipulated, ambient seawater (i.e., treatment seawater conditions were not at target conditions until incubation 6) during incubations 1–5 (up to 144 mmol photons m^{-2} h^{-1}; Fig. 2a). NCP rates ranged between 30 and 45 μmol O_2 g dw^{-1} h^{-1} when PAR was ≥80 mmol photons m^{-2} h^{-1}, which occurred during incubations 1–5. Incubations 6–12 displayed a linear response between measured rates of NCP and irradiance—PAR never exceeded 40 mmol photons m^{-2} h^{-1} during these incubations (Fig. 2b). The observed PAR during incubations 6–12, when the treatment mesocosms were at target conditions, was lowest in the MSH treatment, which yielded a maximum flux of 22 mmol photons m^{-2} h^{-1}, and highest in the control and HT treatments, which recorded values of 37 mmol photons m^{-2} h^{-1}. This greater PAR flux resulted in slightly higher measured rates of NCP for the control and HT treatments.

Incubation 7 was excluded from this analysis as the recorded O_2, temperature, salinity, and the associated metadata from the system were not logged due to a communication error with the server from 2021-07-21 08:01 to 2021-07-26 12:37 UTC. This happened despite successful regulation of the experimental conditions and the continued display of real-time measured data in each of the mesocosms on the interface, during this period. Incubation 8 was also removed from the analysis as erroneous O_2 measurements were recorded due to a circuit failure causing the 12 W wave pumps inside each mesocosm to shut off for ~36–48 h. This prevented the water in each mesocosm from being thoroughly mixed leading to the erroneous measurements.

The linear modeled P—I response for incubations 6–12 displayed non-statistically significant differences between the 3 different treatments and the control for all parameters (Fig. 3). Due to the fractional factorial design of the experiment, only comparisons against the control were directly assessed as inter-treatment comparisons were confounded by differing multi-perturbing predictor variables. The mean photosynthetic efficiency derived from the predicted parameter (α) from each treatment's linear model was estimated to be 0.882 ± 0.209 (SD) (μmol O_2 g dw^{-1} h^{-1} (mmol photons m^{-2} h^{-1})$^{-1}$) with an I_c of 13.61 ± 1.66 (SD) mmol photons m^{-2} h^{-1} (Fig. 3). This I_c equates to a continuous instantaneous flux of 3.78 μmol m^{-2} s^{-1}. All predicted model parameters (slope and intercept) were significant for each treatment condition (ANOVA of linear model, p-value <0.0001). The overall predicted rate by the models shared considerable overlap of the RMSE bounds (Fig. 3b). The similarity between treatments suggest a robust estimation of NCP rates as a linear response to irradiance when the flux was <40 mmol photons m^{-2} h^{-1}.

The integrated sum (i.e., the sum of all measured hourly rates over the entire experiment) of the net community production displayed non-significant differences between the treatments and the control (Fig. 4a). All treatments had a mean value that ranged between 0.4 and 0.55 mmol O_2 g dw^{-1}. The calculated integrated sum for incubations 6–12 (i.e., when at treatment conditions), showed a significant difference between the control and the MSH treatment (rank-sum, p-value = 0.0487) (Fig. 4b). The total net community production based on the integrated sum was 121 μmol O^2 g dw^{-1} for the control and − 66.6 μmol O^2 g dw^{-1} for the MSH treatment. The comparison of the integrated sum of net community production for the model predicted rates for 5 'typical light days' displayed no differences between treatments and the control.

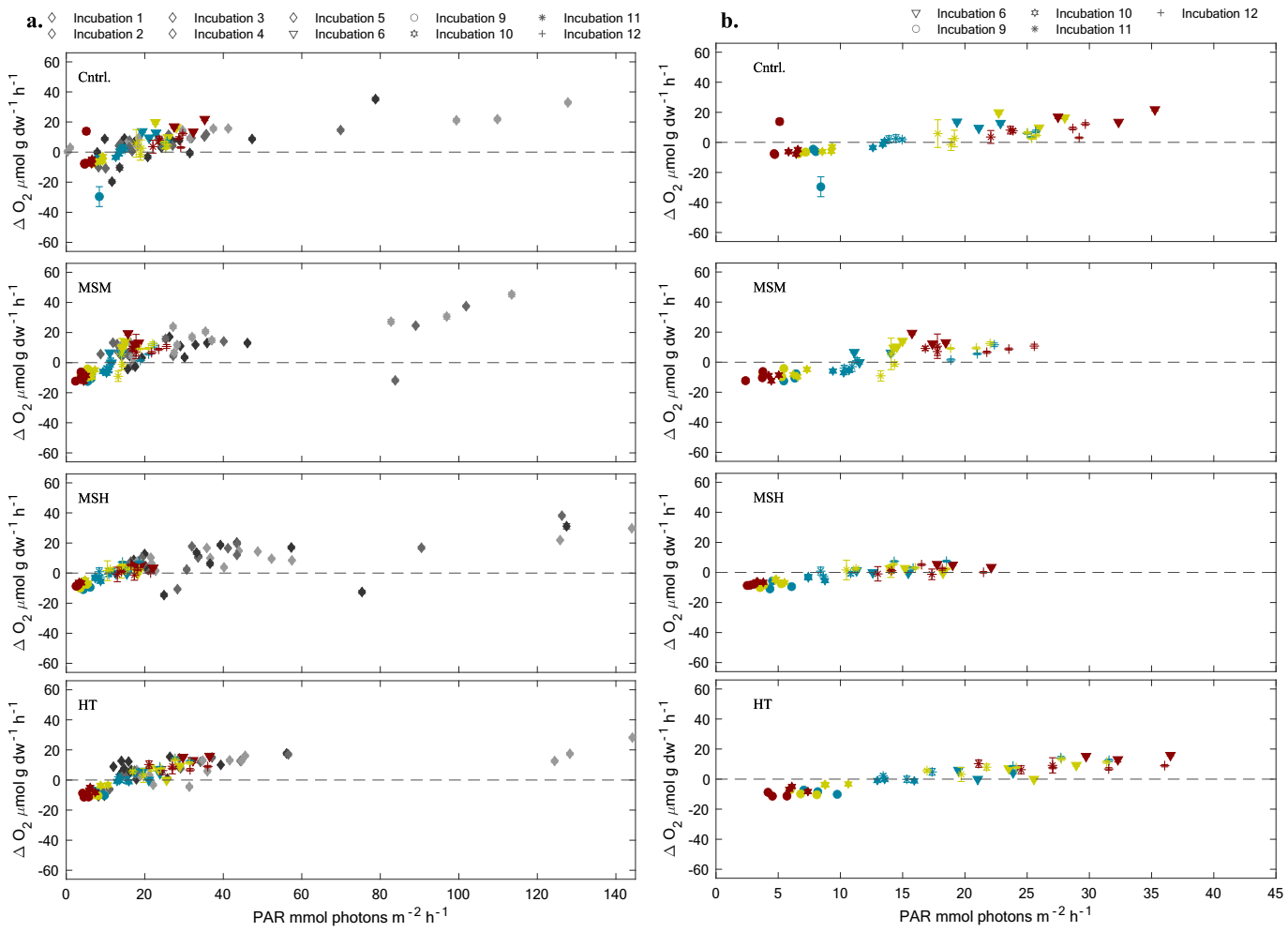

Fig. 2. Rates of net community productivity for all incubations: (a) incubations 1–12, and (b) incubations 6–12. Incubations 1–5 occurred while all mesocosms were at ambient conditions (panel a, grey markers). Incubations 6–12 (colored markers panel a and b) were conducted when all treatment conditions were at target temperature, salinity, and irradiance. Different symbols represent different incubations where blue is replicate 1, yellow is replicate 2, and red is replicate 3. Date and times (UTC) for each incubation are as follows. Incubation 1: 2021-07-04 04:18–07:20; Incubation 2: 2021-07-05 17:30–20:30; Incubation 3: 2021-07-06 10:18–13:18; Incubation 4: 2021-07-08 04:02–07:02; Incubation 5: 2021-07-09 08:49–11:49; Incubation 6: 2021-07-16 04:30–07:30; Incubation 9: 2021-08-06 17:40–20:42; Incubation 10: 2021-08-13 17:09–20:10; Incubation 11: 2021-08-20 04:16–07:20; Incubation 12: 2021-08-26 09:41–12:38.

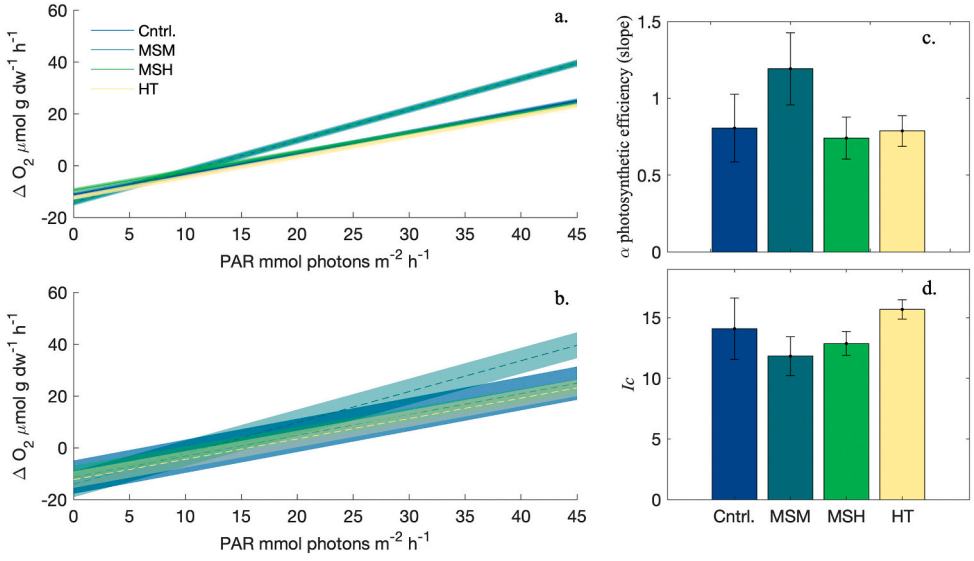

Fig. 3. (a) Slope of model for each individual treatment (error is RSMSE) and (b) the whole model of net community productivity rate by treatment with RMSE. Bar charts are the associated model parameters: (c) photosynthetic efficiency and (d) compensation irradiance (error is 95 % CI).

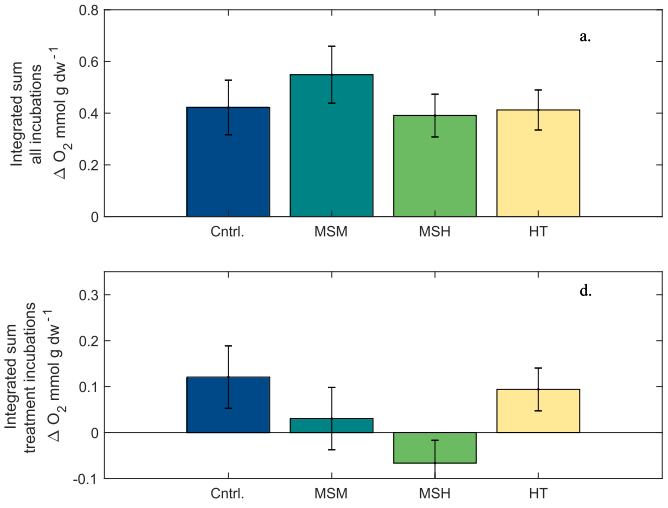

Fig. 4. (a) Integrated sum of all hourly NCP rates for all incubations (i.e., incubations 1–12). (b) Integrated sum of all hourly NCP rates for incubations 6–12 (time period when all treatments were at target conditions). Error bars are the 95 % CI.

(Fig. S4).

3.3. Carbonate chemistry variability of treatment conditions

The change in pH_T (and $[H^+]$) as a response to the NCP rate displayed a robust fit (all $R^2 > 0.9$) with 2nd (MSH treatment) and 3rd (Cntrl., MSM, HT) order polynomials (Fig. S5). Discrete bottle estimates for pH_T were valid for incubations 2–12 (excluding incubation 8). Several anomalous values were measured in both the T_0 and T_f discrete A_T bottles resulting in a lack of confidence in deriving the change of independent carbonate chemistry parameters over the duration of an incubation. Thus, determination of changes in A_T and C_T during an incubation are not reported. Valid A_T samples (see Section 2.3) were sufficient enough to determine an A_T:C_T ratio that ranged from 1.09 to 1.19 across all treatment conditions using a subset of the robust T_0 values—thus the baseline A_T:C_T state for each treatment.

The degree of change in pH_T as a function of net kelp community productivity over an incubation period was modeled with 2nd and 3rd polynomials from the starting mean pH_T condition at T_0 for each treatment condition (Fig. 5). The difference between the measured starting point of pH_T for each condition was dependent on the A_T:C_T ratio and described by the thermodynamic response of the carbonate system to temperature and salinity. The lowest A_T:C_T was found in the MSH treatment; thus, this condition experienced the greatest change in pH_T as a response to the rate of NCP (Fig. 5).

3.4. Effect of covariates on NCP

The explanatory variables PAR, 'Time of day,' and 'Day of year' appeared to have significant effects on NCP rates for incubations 6–12 (Table S2). The covariate 'Time of day' had a significant negative effect ($F_{1,165} = 14.2$; p-value $= 0.0002$) on NCP rates, however, there was a significant interaction effect with irradiance (Fig. S5). The 'Day of year' covariate was also statistically significant ($F_{1,165} = 14.2$; p-value $= 0.0122$) (Table S2). The significant positive effect of the 'Day of year' on rates of NCP was likely due to higher irradiance during incubations conducted toward the beginning of the experiment (Fig. S6). This was not the case for the 'Time of day' effect, however, as the decrease in NCP rate was shown to be steady as the day increased (Fig. S6). Evidence is visible when looking at mid-day (~ 12:00 h local time) NCP rates and

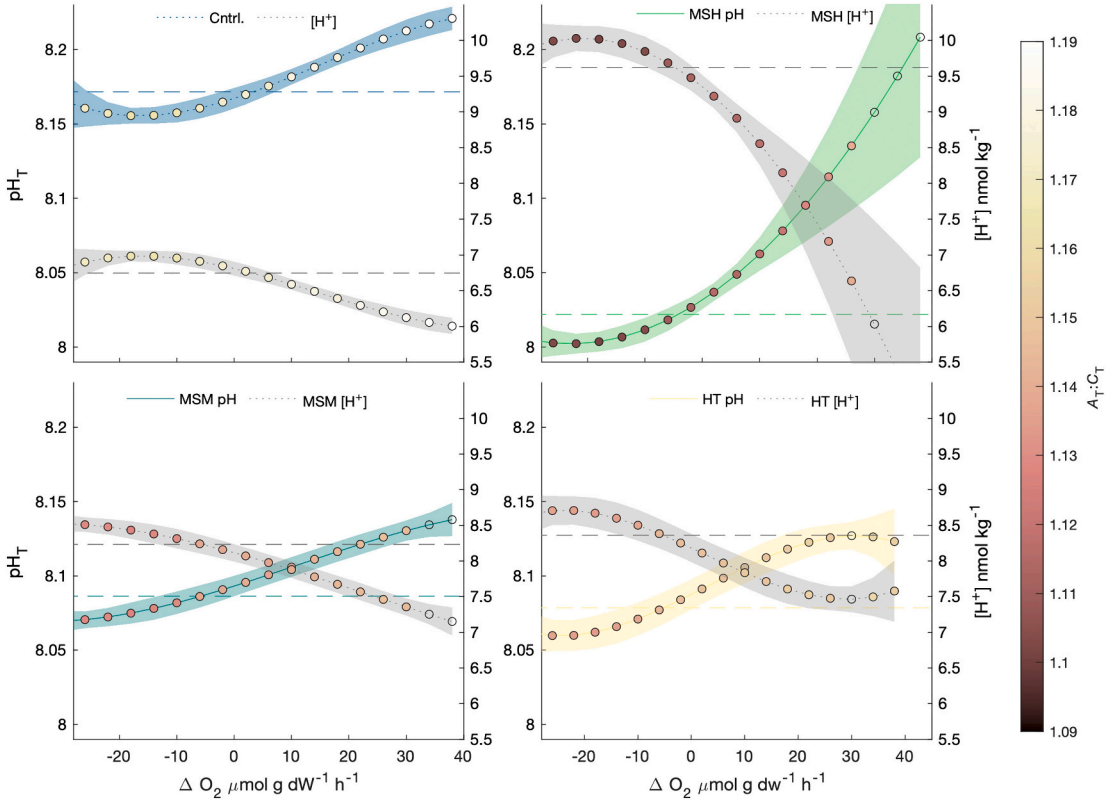

Fig. 5. Modeled response of change in pH_T and $[H^+]$ by treatment as a function of NCP rate. Dashed colored lines show mean pH_T across replicates (and within a treatment) at T_0 for incubations 6–12. Dashed grey lines show the mean $[H^+]$ across replicates (and within a treatment) at T_0 for incubations 6–12. Bounded error is 95 % CI. Filled colored circles represent the starting A_T:C_T ratio.

the moderate irradiance levels compared to those earlier in the day. The PAR covariate had the largest effect on NCP rate ($F_{1,165} = 106.3$; p-value <0.0001). No difference in NCP rates were observed between treatment conditions (Table S2), corroborating the overlap of the estimated rates observed in the individual model predictions.

3.5. Pooled model and community production

The estimated net kelp community productivity had a P_{max} (maximum NCP rate) coefficient of 32 μmol O_2 g dw^{-1} h^{-1} at a saturating irradiance of 150 mmol photons m^{-2} h^{-1}. The modified hyperbolic tangent model (Eq. (1)) provided a robust fit with an RMSE of 5.73 μmol O_2 g dw^{-1} h^{-1} (Fig. 6). The normative hyperbolic tangent model (photosynthesis-irradiance only) suggested a higher photosynthetic efficiency and resulted in a less robust fit with an RMSE of 6.39 μmol O_2 g dw^{-1} h^{-1}. The modified hyperbolic tangent model predicted a respiration rate coefficient of −13.1 μmol O_2 g dw^{-1} h^{-1} which was ~40 % higher than that of the non-modified hyperbolic tangent model (- 9.4 μmol O_2 g dw^{-1} h^{-1}). This aligned well with the measured respiration rates which ranged from −21 to −11 O_2 g dw^{-1} h^{-1} over a 3 h period (Fig. S7).

The estimated net community production for a proportion of the summer season (57 d period) in Kongsfjorden—which utilized the irradiance measured in a control mesocosm—ranged from −25 to 128 mmol O_2 m^{-2} d^{-1} (Fig. 7). Maximum net community production occurred during the first week of July, while several net negative rates were observed the last week of August. The overall trend was linear and showed a decrease in production over the modeled period representative of the decreasing irradiance over this time. Overall, the modeled period displayed that mixed kelp communities experience net positive production 91 % of the time with irradiance values measured at a simulated 10 m depth.

4. Discussion

4.1. Tolerance of mixed kelp communities

This study has shown that mixed kelp communities in an Arctic fjord exposed to varying degrees of multi-stressors appear tolerant to future environmental conditions. Utilizing a novel experimental system to manipulate seawater temperature and salinity while reducing light availability (Miller et al., 2024), this study documents a retained capacity for productivity by mixed kelp sporophyte assemblages under a large range of conditions, and the most extreme mean temperatures predicted for the Arctic by the year 2100. The nearly two-month long experiment showed that NCP rates and their photosynthetic efficiency were similar across all experimental conditions during the 54 d exposure. Importantly, we show that the 'Time of day' is an additional covariate affecting production and should be considered when assessing the photosynthetic capacity of Arctic kelp, despite the fact that polar days potentially provide continual saturating irradiance. To our knowledge, this is the first account to quantify the NCP response of mixed kelp communities in the Arctic to a range of multiple driver scenarios, all of which are plausible to occur in future high latitude fjord systems.

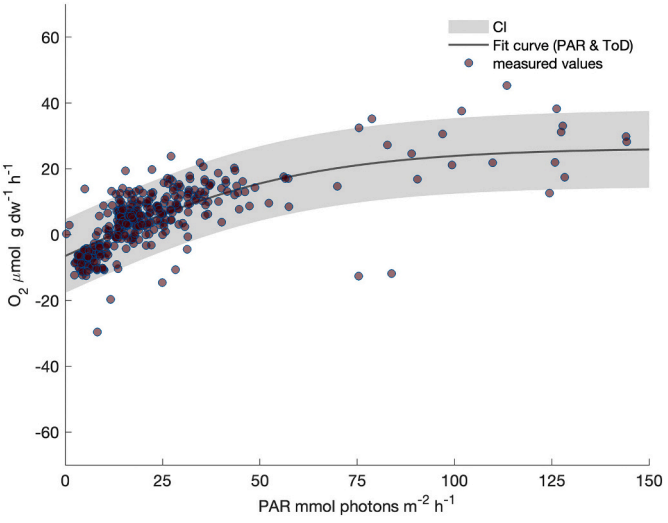

Fig. 6. Modified hyperbolic tangent function (Eq. (1)) of predicted NCP rate with a median 'Time of day'. Modeled bounds are 95 % CI and individual points are measured rates of hourly NCP.

The response of Arctic kelp sporophytes to individual stressors has been well documented, with indications that increased temperatures may be favorable during reproduction and growth, whereas turbidity appears to have the strongest negative effect (Filbee-Dexter et al., 2019; Lebrun et al., 2022). While there was no clear indication of a temperature effect (at up to +5.3 °C from ambient) on the production capacity of mixed communities in this study, the effect of the MSH treatment showed evidence of a potential decrease in the overall accumulated production when looking at the integrated sum of hourly NCP over the entire experimental period. Even though the modeled NCP rates displayed non-significant differences of the treatments, which was further corroborated by a non-significant treatment effect, it appears that the extremes of the MSH treatment were likely at the threshold of physiological tolerance for the mixed kelp communities. The slight significant difference in the integrated sum of hourly NCP between the control and the MSH treatment can likely be explained by PAR values ranging between 11 and 14 mmol photons m^{-2} h^{-1} (i.e., ± 12 % the estimated I_c) for 11 % of the observations in the MSH treatment. With the additional limiting effect of 'Time of day' on NCP, this could have resulted in the accumulation of more negative than positive rates around these PAR levels. While the results here appear contrary to the clear evidence that shows that increased turbidity (i.e., attenuated light) and freshening reduce the photosynthetic capacity of kelp, it is important to consider the duration and magnitude of these stressors. Indeed, extremely low salinities (⟨10) have been shown to cause a decreased photosynthetic capacity for the same species tested in this study (Karsten, 2007), and increased turbidity reduces the annual productive capacity of kelp in the Arctic (Bonsell and Dunton, 2018), but the short-term tolerance of kelp to the stressors evaluated in this study demonstrate the importance of duration and recovery time. Future aims should, thus, track the long-term effects of the exposure presented in this study by assessing the resilience of kelp during the dark winter season and its growth potential at first light in the following season following such summertime perturbations.

The results of this study suggest that short-term exposure to multi-stressors does not appear to have an additive, negative, or synergistic effect on kelp communities. This can be seen as a positive outlook for Arctic kelp communities confronting the consortium of future environmental changes. The long-term effects of this exposure, however, remain uncertain, and the impact of the most extreme drivers tested here (MSH treatment) should be further investigated such as increased exposure period or variability in perturbation magnitudes. Based on this study, it is unfeasible to forecast if the potential decrease in accumulated net positive rates observed in our treatment conditions (MSM and MSH) translates to a reduced storage of energy (e.g., laminarin) reserves in the form of carbohydrates and lipids, which are needed to carry the organism through the dark winter season (Borum et al., 2002). Gordillo et al. (2022) showed that two of the three species examined in this study (*A. esculenta* and *S. latissima*) were unable to recover their O_2 evolution potential over a 7-d photoperiod at the cessation of the winter period, when temperature was artificially increased by +8 °C. This is not to say that these kelp species are not resilient with respect to surviving dark winter periods, as studies have shown that the photosynthetic

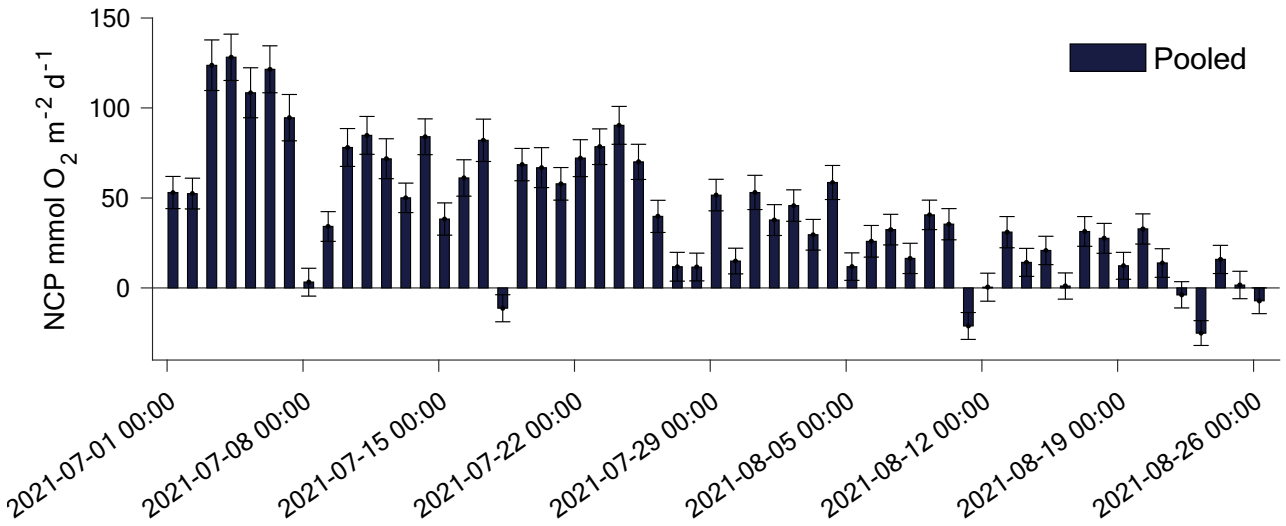

Fig. 7. Estimated net community production of mixed kelp communities using measured PAR values simulating spectra and irradiance at 10 m depth. Estimates derived from hyperbolic tangent model (Eq. (1)) with 95 % CI.

competency is sustained during the winter darkness (Gordillo et al., 2022; Scheschonk et al., 2019). What is of relevance, is the magnitude of warm water exposure, at least during the winter period, which appears to negatively affect kelp communities in the Arctic. With respect to this, longer term research is needed, potentially tracking the accumulation and storage of these biomolecules through the dark winter season, including the O_2 evolution capacity upon the return of light. This is particularly relevant considering that the magnitude of warming will vary seasonally, meaning that future warming scenarios predict higher temperatures at the end of summer compared to months at the end of winter (Meredith et al., 2019). Evidence may suggest, however, that the retention of these bioenergy stores remain adequate as additional analyses associated with this study found non-significant differences in C:N across the experimental conditions at the end of the study period (Lebrun et al., 2023).

4.2. Estimated kelp production

This study provides some of the first robust estimates of mixed kelp NCP in an Arctic fjord, an area of study that is significantly lacking despite recent estimates quantifying coarse, global scale net primary production by macroalgae (Duarte et al., 2022; Pessarrodona et al., 2022). The findings here align well with individual studies on two of the three species sampled (*S. latissima* and *A. esculenta*), which displayed non-significant differences in net photosynthetic rates across a temperature range of 3 to 11 °C when individually incubated (Niedzwiedz and Bischof, 2023). There are limitations to our estimates, however, due to the logistics of properly replicating in-situ communities with an ex-situ mesocosm experiment. This may include an underrepresentation of the metabolic signatures of the infaunal community and microphytobenthos, which have been shown to contribute significantly to benthic metabolic fluxes (Sevilgen et al., 2014). Despite these limitations, the present study provides a substantial baseline estimate for the capacity and contribution of macroalgae production now, and into the future.

The constructed NCP rate model presented here suggests that the mixed kelp communities experience an I_c between 12 and 12.5 mmol photons m^{-2} h^{-1} at the median 'Time of day' (a continuous instantaneous flux of 3.33–3.41 μmol photons m^{-2} s^{-1}). The effect of 'Time of day' can shift this I_c value by 8 mmol photons m^{-2} h^{-1}, according to the model estimates (Fig. 8). It may be more realistic, however, to think of 'Time of day' as cumulative hours above the compensation point. This estimate is crucial when placed in the context of rapidly changing

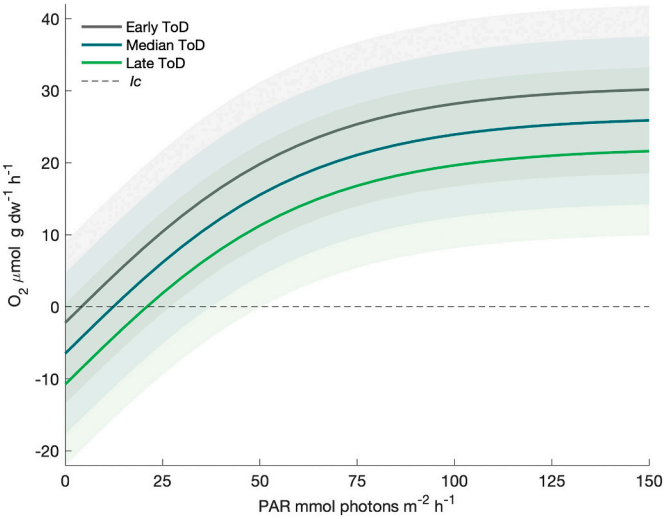

Fig. 8. Modeled compensation irradiance point at an early, median, and late 'Time of day' (ToD) effect. In decimal hours this 0.168 (Early ToD), 0.493 (Median ToD), 0.819 (Late ToD).

underwater light conditions in nearshore Arctic systems. This estimate is similar to those found for the same species in another study (Niedzwiedz and Bischof, 2023). While this provides corroborated evidence for the production capacity of benthic kelp communities in Kongsfjorden, it is difficult to determine the regional limits of potential kelp expansion within the fjord and, thus, the total contribution to ecosystem productivity. The prediction of regional depth limitation is necessary to determine how the expansion or contraction of these kelp assemblages may impact benthic primary production within the fjord and, thus, a model for other fjord systems. While daily oxygen budgets have been determined for soft-bottomed microphytobenthic communities in Kongsfjorden (Sevilgen et al., 2014), these estimates suggest a heterotrophic net community production, while in this study, we estimate that net community production by mixed kelp communities is autotrophic >90 % of the 57 d modeled. Our estimates show similar values (assuming a photosynthetic quotient of 1:1) to estimated net community production for kelp off the coast of New Zealand in early spring and fall at a 14 m depth (Rodgers and Shears, 2016). Based on this, kelp community productivity in Kongsfjorden and throughout the Arctic may

contribute substantially to ecosystem metabolism and function. The response of this vigorous production by kelp communities in the fjord demonstrates a gap in knowledge of how this metabolic signal affects the movement of nutrients and biogeochemical cycling within the fjord, thus impacting system function.

One potential factor thought to potentially support macrophyte expansion in the Arctic are long photoperiods (Sanz-Martín et al., 2019). The daily production determined from this study found that despite the potential for nearly day-long saturating irradiance (~ 1.5 mol photons m^{-2} d^{-1} derived from the model in this study), the mixed kelp assemblages maintained a natural biorhythm, or at least a decrease in production as the day evolved. Many Arctic kelp come from a boreal origin, which could possibly explain this observation (Bringloe et al., 2020; Wulff et al., 2009). The negative correlation found with NCP and 'Time of day' suggests that there may not be a continual need to produce carbohydrates throughout the day and into the next. While the exact mechanism driving a reduction in photosynthesis later in a 24 h day is unknown, this effect should be investigated further given the implication this could have on kelp, their assemblage composition, and their expansion into the Arctic.

5. Conclusion

The ability of mixed kelp communities in Kongsfjorden to tolerate future climate extremes while remaining productive has been presented in this study. While the long-term effects of such stress cannot be determined, we show a marked capacity by mixed sporophyte kelp communities to manage high degrees of multi-stressors. Turbidity effects (i.e., attenuated light) appeared to be the dominant stressor in this study which presented as a reduced integrated sum of cumulative hourly NCP for the most extreme treatment condition. This effect is yet to be seen as potentially detrimental, however, and needs further investigation. While this study captured 54 d of the summer season, early production and physiological function of kelp communities in the spring season remain unknown. Determining the total period of kelp production will help to understand how energy stores are accumulated and support the yearly production of kelp assemblages, as well as their contribution to ecosystem production.

Despite the resilience of kelp to multi-stressors presented here, previous studies have clearly shown that the sporophyte life-stage responds differently to a stress, such as temperature when compared to the germination process and the gametophyte stage (Filbee-Dexter et al., 2019; Wiencke and Clayton, 2002). In this study we tested only adult sporophytes, and this distinction should be noted when discussing the resilience of Arctic kelp communities to future climate stressors. While we examined the effect of reduced irradiance caused by turbidity, we did not account for turbidity effect of increased benthic sedimentation which has been shown to inhibit recruitment (Zacher et al., 2016). There is evidence, however, to suggest that the magnitude of warming in the Arctic could enhance germination rates, and physiological studies have shown that kelp gametophytes are tolerant to long periods of darkness which could increase with enhanced Arctic turbidity (Bartsch et al., 2008; Sjøtun and Schoschina, 2002).

Whether or not Arctic kelp communities will expand as predicted by some studies (Assis et al., 2022; Krause-Jensen et al., 2020), it is determined here that the projected extreme changes are at least tolerated within the experimental limit of stress from the standpoint of photosynthetic production. Expansion of such mixed kelp communities in the Arctic suggests a resilience rather than a tolerance under future Arctic conditions. With respect to this, more studies are needed to corroborate these Pan-Arctic model projections. A better understanding of how species distribution and competition for space needs to be considered as these ecological interactions can impact where, and how, Arctic kelp expansion may occur (Goldsmit et al., 2021; Moreno, 2015).

CRediT authorship contribution statement

Cale A. Miller: Data curation, Formal analysis, Investigation, Methodology, Writing – original draft. **Frédéric Gazeau:** Conceptualization, Writing – review & editing. **Anaïs Lebrun:** Data curation. **Jean-Pierre Gattuso:** Conceptualization, Investigation, Project administration, Supervision, Writing – review & editing. **Samir Alliouane:** Investigation, Methodology. **Pierre Urrutti:** Methodology, Resources. **Robert W. Schlegel:** Investigation, Writing – review & editing. **Steeve Comeau:** Conceptualization, Investigation, Methodology, Writing – review & editing.

Declaration of competing interest

The authors declare no competing interests exist.

Data availability

Data supporting the findings of this study are openly avaialble on the *PANGAEA* platform: Miller, Cale A; Gazeau Frédéric; Lebrun, Anais; Gattuso, Jean-Pierre; Alliouane, Samir; Urrutti, Pierre; Schlegel, Robert; Comeau, Steeve (2024); Net communtiy prodcution of Arctic mixed kelp communties in response to warming, freshening, and attenuated light: a mesocosm study as per minute record [dataset]. *PANGAEA:* http://doi.pangaea.de/10.1594/PANGAEA.967056.

Acknowledgements

This study is part of the FACE-IT Project (The Future of Arctic Coastal Ecosystems – Identifying Transitions in Fjord Systems and Adjacent Coastal Areas). The authors thank Simon Jungblut for helping with the breakdown of the experiment, Jens Terhaar for helping with temperature projection data, Philipp Fischer for access to the AWIPEV data, the AWI dive team, and the AWIPEV and Kings Bay staff for helping with logistical details, shipping, and access to marine lab facilities.

Financial support

FACE-IT has received funding from the European Union's Horizon 2020 research and innovation programme under grant agreement no. 869154. Partial financial support was provided by IPEV, The French Polar Institute.

Appendix A. Supplementary data

Supplementary data to this article can be found online at https://doi.org/10.1016/j.scitotenv.2024.172571.

References

Abdullah, M.I., Fredriksen, S., Christie, H., 2017. The impact of the kelp (Laminaria hyperborea) forest on the organic matter content in sediment of the west coast of Norway. Mar. Biol. Res. 13 (2), 151–160. https://doi.org/10.1080/17451000.2016.1240369.

Alongi, D.M., 2018. Kelp forests. In: Alongi, D.M. (Ed.), Blue Carbon: Coastal Sequestration for Climate Change Mitigation. Springer International Publishing, pp. 53–57. https://doi.org/10.1007/978-3-319-91698-9_5.

Asbjørnsen, H., Årthun, M., Skagseth, Ø., Eldevik, T., 2020. Mechanisms underlying recent Arctic Atlantification. Geophys. Res. Lett. 47 (15), e2020GL088036 https://doi.org/10.1029/2020GL088036.

Assis, J., Serrão, E.A., Duarte, C.M., Fragkopoulou, E., Krause-Jensen, D., 2022. Major expansion of marine forests in a warmer Arctic. Front. Mar. Sci. 9 https://doi.org/10.3389/fmars.2022.850368.

Attard, K.M., Hancke, K., Sejr, M.K., Glud, R.N., 2016. Benthic primary production and mineralization in a High Arctic fjord: in situ assessments by aquatic eddy covariance. Mar. Ecol. Prog. Ser. 554, 35–50. https://doi.org/10.3354/meps11780.

Bartsch, I., Wiencke, C., Bischof, K., Buchholz, C.M., Buck, B.H., Eggert, A., Feuerpfeil, P., Hanelt, D., Jacobsen, S., Karez, R., Karsten, U., Molis, M., Roleda, M.Y., Schubert, H., Schumann, R., Valentin, K., Weinberger, F., Wiese, J., 2008. The genus Laminaria sensu lato: recent insights and developments. Eur. J. Phycol. 43 (1), 1–86. https://doi.org/10.1080/09670260701711376.

Bartsch, I., Paar, M., Fredriksen, S., Schwanitz, M., Daniel, C., Hop, H., Wiencke, C., 2016. Changes in kelp forest biomass and depth distribution in Kongsfjorden, Svalbard, between 1996–1998 and 2012–2014 reflect Arctic warming. Polar Biol. 39 (11), 2021–2036. https://doi.org/10.1007/s00300-015-1870-1.

Bonsell, C., Dunton, K.H., 2018. Long-term patterns of benthic irradiance and kelp production in the central Beaufort Sea reveal implications of warming for Arctic inner shelves. Prog. Oceanogr. 162, 160–170. https://doi.org/10.1016/j.pocean.2018.02.016.

Borum, J., Pedersen, M., Krause-Jensen, D., Christensen, P., Nielsen, K., 2002. Biomass, photosynthesis and growth of *Laminaria saccharina* in a high-arctic fjord, NE Greenland. Mar. Biol. 141 (1), 11–19. https://doi.org/10.1007/s00227-002-0806-9.

Bringloe, T.T., Verbruggen, H., Saunders, G.W., 2020. Unique biodiversity in Arctic marine forests is shaped by diverse recolonization pathways and far northern glacial refugia. Proc. Natl. Acad. Sci. 117 (36), 22590–22596. https://doi.org/10.1073/pnas.2002753117.

Carvalho, K.S., Wang, S., 2020. Sea surface temperature variability in the Arctic Ocean and its marginal seas in a changing climate: patterns and mechanisms. Glob. Planet. Chang. 193, 103265 https://doi.org/10.1016/j.gloplacha.2020.103265.

Chen, J.-L., Kang, S.-C., Meng, X.-H., You, Q.-L., 2019. Assessments of the Arctic amplification and the changes in the Arctic sea surface. Adv. Clim. Chang. Res. 10 (4), 193–202. https://doi.org/10.1016/j.accre.2020.03.002.

Dickson, A., 1990. Thermodynamics of the dissociation of boric-acid in synthetic seawater from 273.15-K to 318.15-K. Deep-Sea Res. A-Oceanogr. Res. Pap. 37 (5), 755–766. https://doi.org/10.1016/0198-0149(90)90004-F.

Dickson, A.G., Sabine, C.L., Christian, J.R., 2007. Guide to Best Practices for Ocean CO_2 Measurements. [Report]. North Pacific Marine Science Organization. http://www.oceandatapractices.net:80/handle/11329/249.

Duarte, C.M., Gattuso, J.-P., Hancke, K., Gundersen, H., Filbee-Dexter, K., Pedersen, M. F., Middelburg, J.J., Burrows, M.T., Krumhansl, K.A., Wernberg, T., Moore, P., Pessarrodona, A., Ørberg, S.B., Pinto, I.S., Assis, J., Queirós, A.M., Smale, D.A., Bekkby, T., Serrão, E.A., Krause-Jensen, D., 2022. Global estimates of the extent and production of macroalgal forests. Glob. Ecol. Biogeogr. 31 (7), 1422–1439. https://doi.org/10.1111/geb.13515.

Filbee-Dexter, K., Wernberg, T., Norderhaug, K.M., Ramirez-Llodra, E., Pedersen, M.F., 2018. Movement of pulsed resource subsidies from kelp forests to deep fjords. Oecologia 187 (1), 291–304. https://doi.org/10.1007/s00442-018-4121-7.

Filbee-Dexter, K., Wernberg, T., Fredriksen, S., Norderhaug, K.M., Pedersen, M.F., 2019. Arctic kelp forests: diversity, resilience and future. Glob. Planet. Chang. 172, 1–14. https://doi.org/10.1016/j.gloplacha.2018.09.005.

Fox-Kemper, B., Hewitt, H.T., Xiao, C., Aðalgeirsdóttir, G., Drijfhout, S.S., Edwards, T.L., Golledge, N.R., Hemer, M., Kopp, R.E., Krinner, G., Mix, A., Notz, D., Nowicki, S., Nurhati, I.S., Ruiz, L., Sallée, J.-B., Slangen, A.B.A., Yu, Y., 2021. Ocean, cryosphere, and sea level change. In V. Masson-Delmotte. In: Zhai, P., Pirani, A., Connors, S.L., Péan, C., Berger, S., Caud, N., Chen, Y., Goldfarb, L., Gomis, M.I., Huang, M., Leitzell, K., Lonnoy, E., Matthews, J.B.R., Maycock, T.K., Waterfield, T., Yelekçi, Ö., Yu, R., Zhou, B. (Eds.), Climate Change 2021: The Physical Science Basis. Contribution of Working Group I to the Sixth Assessment Report of the Intergovernmental Panel on Climate Change. Cambridge University Press, pp. 1211–1362. https://doi.org/10.1017/9781009157896.001.

Fragkopoulou, E., Serrão, E.A., De Clerck, O., Costello, M.J., Araújo, M.B., Duarte, C.M., Krause-Jensen, D., Assis, J., 2022. Global biodiversity patterns of marine forests of brown macroalgae. Glob. Ecol. Biogeogr. 31 (4), 636–648. https://doi.org/10.1111/geb.13450.

Fransson, A., Chierici, M., Hop, H., Findlay, H.S., Kristiansen, S., Wold, A., 2016. Late winter-to-summer change in ocean acidification state in Kongsfjorden, with implications for calcifying organisms. Polar Biol. 39 (10), 1841–1857. https://doi.org/10.1007/s00300-016-1955-5.

Fredriksen, S., Karsten, U., Bartsch, I., Woelfel, J., Koblowsky, M., Schumann, R., Moy, S. R., Steneck, R.S., Wiktor, J.M., Hop, H., Wiencke, C., 2019. Biodiversity of benthic macro- and microalgae from Svalbard with special focus on Kongsfjorden. In: Hop, H., Wiencke, C. (Eds.), The Ecosystem of Kongsfjorden, Svalbard. Springer International Publishing, pp. 331–371. https://doi.org/10.1007/978-3-319-46425-1_9.

Gattuso, J.-P., Alliouane, S., Fischer, P., 2023. High-frequency, year-round time series of the carbonate chemistry in a high-Arctic fjord (Svalbard). Earth Syst. Sci. Data Discuss. 1–24 https://doi.org/10.5194/essd-2023-92.

Goldsmit, J., Schlegel, R.W., Filbee-Dexter, K., MacGregor, K.A., Johnson, L.E., Mundy, C.J., Savoie, A.M., McKindsey, C.W., Howland, K.L., Archambault, P., 2021. Kelp in the eastern Canadian Arctic: current and future predictions of habitat suitability and cover. Front. Mar. Sci. 8 https://doi.org/10.3389/fmars.2021.742209.

Gordillo, F.J.L., Carmona, R., Jiménez, C., 2022. A warmer Arctic compromises winter survival of habitat-forming seaweeds. Front. Mar. Sci. 8 https://doi.org/10.3389/fmars.2021.750209.

Hegseth, E.N., Assmy, P., Wiktor, J.M., Wiktor, J., Kristiansen, S., Leu, E., Tverberg, V., Gabrielsen, T.M., Skogseth, R., Cottier, F., 2019. Phytoplankton seasonal dynamics in Kongsfjorden, Svalbard and the adjacent shelf. In: Hop, H., Wiencke, C. (Eds.), The Ecosystem of Kongsfjorden, Svalbard. Springer International Publishing, pp. 173–227. https://doi.org/10.1007/978-3-319-46425-1_6.

Hop, H., Wiencke, C., Vögele, B., Kovaltchouk, N.A., 2012. Species composition, zonation, and biomass of marine benthic macroalgae in Kongsfjorden, Svalbard. Bot. Mar. 55 (4), 399–414. https://doi.org/10.1515/bot-2012-0097.

Hop, H., Cottier, F., Berge, J., 2019. Autonomous Marine Observatories in Kongsfjorden, Svalbard. In: Hop, H., Wiencke, C. (Eds.), The Ecosystem of Kongsfjorden, Svalbard. Springer International Publishing, pp. 515–533. https://doi.org/10.1007/978-3-319-46425-1_13.

Husum, K., Howe, J.A., Baltzer, A., Forwick, M., Jensen, M., Jernas, P., Korsun, S., Miettinen, A., Mohan, R., Morigi, C., Myhre, P.I., Prins, M.A., Skirbekk, K., Sternal, B., Boos, M., Dijkstra, N., Troelstra, S., 2019. The marine sedimentary environments of Kongsfjorden, Svalbard: an archive of polar environmental change. Polar Res. https://doi.org/10.33265/polar.v38.3380.

Karsten, U., 2007. Research note: salinity tolerance of Arctic kelps from Spitsbergen. Phycol. Res. 55 (4), 257–262. https://doi.org/10.1111/j.1440-1835.2007.00468.x.

Konik, M., Darecki, M., Pavlov, A.K., Sagan, S., Kowalczuk, P., 2021. Darkening of the Svalbard fjords waters observed with satellite ocean color imagery in 1997–2019. Front. Mar. Sci. 8 https://doi.org/10.3389/fmars.2021.699318.

Krause-Jensen, D., Archambault, P., Assis, J., Bartsch, I., Bischof, K., Filbee-Dexter, K., Dunton, K.H., Maximova, O., Ragnarsdóttir, S.B., Sejr, M.K., Simakova, U., Spiridonov, V., Wegeberg, S., Winding, M.H.S., Duarte, C.M., 2020. Imprint of climate change on pan-Arctic marine vegetation. Front. Mar. Sci. 7 https://doi.org/10.3389/fmars.2020.617324.

Lebrun, A., Comeau, S., Gazeau, F., Gattuso, J.-P., 2022. Impact of climate change on Arctic macroalgal communities. Glob. Planet. Chang. 219, 103980 https://doi.org/10.1016/j.gloplacha.2022.103980.

Lebrun, A., Miller, C.A., Meynadier, M., Comeau, S., Urrutti, P., Alliouane, S., Schlegel, R., Gattuso, J.-P., Gazeau, F., 2023. Multifactorial effects of warming, low irradiance, and low salinity on Arctic kelps. In: EGUsphere (in Review), 1–36. https://doi.org/10.5194/egusphere-2023-1875.

Meire, L., Paulsen, M.L., Meire, P., Rysgaard, S., Hopwood, M.J., Sejr, M.K., Stuart-Lee, A., Sabbe, K., Stock, W., Mortensen, J., 2023. Glacier retreat alters downstream fjord ecosystem structure and function in Greenland. Nat. Geosci. 1–4 https://doi.org/10.1038/s41561-023-01218-y.

Meredith, M., Sommerkon, M., Cassotta, S., Derksen, C., Ekaykin, A., Hollowed, A., Kofinas, G., Mackintosh, A., Melbourne-Thomas, J., Muelbert, M.M.C., Ottersen, G., Ptitchard, H., Schuur, E.A.G., 2019. Chapter 3: Polar regions — Special Report on the Ocean and Cryosphere in a Changing Climate (Polar Regions, pp. 203–320). IPCC. https://www.ipcc.ch/srocc/chapter/chapter-3-2/.

Miller, C.A., Urrutti, P., Gattuso, J.-P., Comeau, S., Lebrun, A., Alliouane, S., Schlegel, R. W., Gazeau, F., 2024. Technical note: an autonomous flow-through salinity and temperature perturbation mesocosm system for multi-stressor experiments. Biogeosciences 21 (1), 315–333. https://doi.org/10.5194/bg-21-315-2024.

Moreno, A.D., 2015. Interspecific competition of sympatric Arctic kelp species under environmental influence [Master]. In: EPIC386 p. https://epic.awi.de/id/eprint/38329/.

Morris, A., Moholdt, G., Gray, L., 2020. Spread of Svalbard glacier mass loss to Barents Sea margins revealed by CryoSat-2. J. Geophys. Res. Earth 125 (8), e2019JF005357. https://doi.org/10.1029/2019JF005357.

Niedzwiedz, S., Bischof, K., 2023. Glacial retreat and rising temperatures are limiting the expansion of temperate kelp species in the future Arctic. Limnol. Oceanogr. 68 (4), 816–830. https://doi.org/10.1002/lno.12312.

Paar, M., de la Vega, C., Horn, S., Asmus, R., Asmus, H., 2019. Kelp belt ecosystem response to a changing environment in Kongsfjorden (Spitsbergen). Ocean Coast. Manag. 167, 60–77. https://doi.org/10.1016/j.ocecoaman.2018.09.003.

Perez, F.F., Fraga, F., 1987. Association constant of fluoride and hydrogen ions in seawater. Mar. Chem. 21 (2), 161–168. https://doi.org/10.1016/0304-4203(87)90036-3.

Pessarrodona, A., Assis, J., Filbee-Dexter, K., Burrows, M.T., Gattuso, J.-P., Duarte, C.M., Krause-Jensen, D., Moore, P.J., Smale, D.A., Wernberg, T., 2022. Global seaweed productivity. Sci. Adv. 8 (37), eabn2465 https://doi.org/10.1126/sciadv.abn2465.

van de Poll, W.H., Maat, D.S., Fischer, P., Visser, R.J.W., Brussaard, C.P.D., Buma, A.G.J., 2021. Solar radiation and solar radiation driven cycles in warming and freshwater discharge control seasonal and inter-annual phytoplankton chlorophyll a and taxonomic composition in a high Arctic fjord (Kongsfjorden, Spitsbergen). Limnol. Oceanogr. 66 (4), 1221–1236. https://doi.org/10.1002/lno.11677.

Rantanen, M., Karpechko, A.Y., Lipponen, A., Nordling, K., Hyvärinen, O., Ruosteenoja, K., Vihma, T., Laaksonen, A., 2022. The Arctic has warmed nearly four times faster than the globe since 1979. Commun. Earth Environ. 3(1), Article 1 https://doi.org/10.1038/s43247-022-00498-3.

Rodgers, K.L., Shears, N.T., 2016. Modelling kelp forest primary production using in situ photosynthesis, biomass and light measurements. Mar. Ecol. Prog. Ser. 553, 67–79. https://doi.org/10.3354/meps11801.

Sanz-Martín, M., Hendriks, I.E., Carstensen, J., Marbà, N., Krause-Jensen, D., Sejr, M.K., Duarte, C.M., 2019. Continuous photoperiod of the artic summer stimulates the photosynthetic response of some marine macrophytes. Aquat. Bot. 158, 103126 https://doi.org/10.1016/j.aquabot.2019.06.005.

Scheschonk, L., Becker, S., Hehemann, J.-H., Diehl, N., Karsten, U., Bischof, K., 2019. Arctic kelp eco-physiology during the polar night in the face of global warming: a crucial role for laminarin. Mar. Ecol. Prog. Ser. 611, 59–74. https://doi.org/10.3354/meps12860.

Schlegel, R., Bartsch, I., Bischof, K., Bjørst, L.R., Dannevig, H., Diehl, N., Duarte, P., Hovelsrud, G.K., Juul-Pedersen, T., Lebrun, A., Merillet, L., Miller, C., Ren, C., Sejr, M., Søreide, J.E., Vonnahme, T.R., Gattuso, J.-P., 2023. Drivers of change in Arctic fjord socio-ecological systems: examples from the European Arctic. Cambridge Prisms Coast. Fut. 1, e13 https://doi.org/10.1017/cft.2023.1.

Sevilgen, D.S., Beer, D. de, Al-Handal, A.Y., Brey, T., Polerecky, L., 2014. Oxygen budgets in subtidal arctic (Kongsfjorden, Svalbard) and temperate (Helgoland, North Sea) microphytobenthic communities. Mar. Ecol. Prog. Ser. 504, 27–42. https://doi.org/10.3354/meps10672.

Sharp, J.D., Pierrot, D., Humphreys, M.P., Epitalon, J.-M., Orr, J.C., Lewis, E.R., Wallace, D.W.R., 2021. *CO2SYSv3 for MATLAB* [computer software]. Zenodo. https://doi.org/10.5281/zenodo.4546015.

Sjøtun, K., Schoschina, E.V., 2002. Gametophytic development of Laminaria spp. (Laminariales, Phaeophyta) at low temperature. Phycologia 41 (2), 147–152. https://doi.org/10.2216/i0031-8884-41-2-147.1.

Skogseth, R., Olivier, L.L.A., Nilsen, F., Falck, E., Fraser, N., Tverberg, V., Ledang, A.B., Vader, A., Jonassen, M.O., Søreide, J., Cottier, F., Berge, J., Ivanov, B.V., Falk-Petersen, S., 2020. Variability and decadal trends in the Isfjorden (Svalbard) ocean climate and circulation – an indicator for climate change in the European Arctic. Prog. Oceanogr. 187, 102394 https://doi.org/10.1016/j.pocean.2020.102394.

Sulpis, O., Lauvset, S.K., Hagens, M., 2020. Current estimates of K_1* and K_2* appear inconsistent with measured CO_2 system parameters in cold oceanic regions. Ocean Sci. 16 (4), 847–862. https://doi.org/10.5194/os-16-847-2020.

Torsvik, T., Albretsen, J., Sundfjord, A., Kohler, J., Sandvik, A.D., Skarðhamar, J., Lindbäck, K., Everett, A., 2019. Impact of tidewater glacier retreat on the fjord system: modeling present and future circulation in Kongsfjorden, Svalbard. Estuar. Coast. Shelf Sci. 220, 152–165. https://doi.org/10.1016/j.ecss.2019.02.005.

Tverberg, V., Skogseth, R., Cottier, F., Sundfjord, A., Walczowski, W., Inall, M.E., Falck, E., Pavlova, O., Nilsen, F., 2019. The Kongsfjorden transect: seasonal and inter-annual variability in hydrography. In: Hop, H., Wiencke, C. (Eds.), The Ecosystem of Kongsfjorden, Svalbard. Springer International Publishing, pp. 49–104. https://doi.org/10.1007/978-3-319-46425-1_3.

Uppström, L.R., 1974. The boron/chlorinity ratio of deep-sea water from the Pacific Ocean. Deep-Sea Res. Oceanogr. Abstr. 21, 161–162. https://doi.org/10.1016/0011-7471(74)90074-6.

Wernberg, T., Krumhansl, K., Filbee-Dexter, K., Pedersen, M.F., 2019. Chapter 3—status and trends for the world's kelp forests. In: Sheppard, C. (Ed.), World Seas: An Environmental Evaluation, Second edition. Academic Press, pp. 57–78. https://doi.org/10.1016/B978-0-12-805052-1.00003-6.

Wiencke, C., Clayton, M.N., 2002. Antarctic Seaweeds. A.R.G. Gantner Verlag. https://www.loc.gov/catdir/toc/fy038/2002507131.html.

Włodarska-Kowalczuk, M., Kukliński, P., Ronowicz, M., Legeżyńska, J., Gromisz, S., 2009. Assessing species richness of macrofauna associated with macroalgae in Arctic kelp forests (Hornsund, Svalbard). Polar Biol. 32 (6), 897–905. https://doi.org/10.1007/s00300-009-0590-9.

Wulff, A., Iken, K., Quartino, M.L., Al-Handal, A., Wiencke, C., Clayton, M.N., 2009. Biodiversity, Biogeography and Zonation of Marine Benthic Micro- and Macroalgae in the Arctic and Antarctic, 52(6), pp. 491–507. https://doi.org/10.1515/BOT.2009.072.

Zacher, K., Bernard, M., Bartsch, I., Wiencke, C., 2016. Survival of early life history stages of Arctic kelps (Kongsfjorden, Svalbard) under multifactorial global change scenarios. Polar Biol. 39 (11), 2009–2020. https://doi.org/10.1007/s00300-016-1906-1.